ACS Photonics

Article

Cite This: ACS Photonics 2018, 5, 3794−3800

pubs.acs.org/journal/apchd5

All-Optical Tunable Microlaser Based on an Ultrahigh-*Q* Erbium-Doped Hybrid Microbottle Cavity

Song Zhu,[†] Lei Shi,*[,†] Bowen Xiao,[†] Xinliang Zhang,[†] and Xudong Fan[§]

[†]Wuhan National Laboratory for Optoelectronics, Huazhong University of Science and Technology, Wuhan 430074, China

[§]Department of Biomedical Engineering, University of Michigan, 1101 Beal Avenue, Ann Arbor, Michigan 48109, United States

Supporting Information

ABSTRACT: An all-optical tunable microlaser based on the ultrahigh-quality (*Q*)-factor erbium-doped hybrid microbottle cavity is proposed and experimentally demonstrated for the first time. All-optical wavelength tunability of the silica microcavity laser is a very attractive feature and has been rarely reported. By using an improved doping method, the erbium-doped silica microbottle cavity with a *Q* factor of 5.2×10^7 in the 1550 nm band is obtained, which is higher than the previous work based on the conventional sol−gel method. Through nonresonant pump in the 980 nm band, a lasing threshold of 1.65 mW is achieved, which is lower than all those realized through the same pump method. Besides, iron oxide nanoparticles are coated on the tapered area by doping them in the ultraviolet curing adhesive in order to precisely control the coating area, which enables the hybrid microcavity to maintain the ultrahigh *Q* factor and possess large tunability. By feeding the control light through the axial direction of the microbottle cavity, the lasing wavelength is all-optically tuned with a range of 4.4 nm, which is larger than the reported doped silica microcavity lasers. This work has great potential in applications such as optical communications, sensing, and spectroscopy.

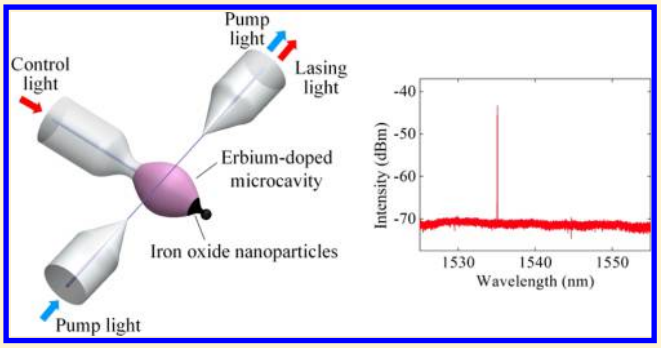

KEYWORDS: *all-optical tuning, microlasers, whispering gallery modes, erbium-doped, iron oxide nanoparticles*

In recent years, due to the advantages of ultralow absorption loss and reflow process induced ultralow surface roughness, silica is selected as one kind of ideal materials for fabricating ultrahigh-quality (*Q*)-factor whispering-gallery-mode (WGM) microcavities.[1−8] Furthermore, the miniature footprint of the WGM microcavity leads to small mode volume, which results in ultrahigh energy density in the microcavity. These excellent features enable it to be utilized in various fundamental and applied research areas, such as cavity quantum electrodynamics,[9,10] optical sensing,[11−15] cavity optomechanics,[5,15] nonlinear optics,[8] and laser emission.[16−20] Especially, silica WGM microcavities exhibit great advantages in ultralow-threshold microlasers, which have potential applications in sensing[18] and communications.[20]

Silica WGM microlasers are based on the undoped or doped microcavities. The undoped microcavity laser is mainly derived from the optical nonlinear effect, such as stimulated Raman scattering[21−24] and stimulated Brillouin scattering.[25,26] Because of the ultrahigh *Q* factor of the silica microsphere, an ultralow-threshold Raman microlaser is first experimentally realized by the Vahala group.[22] On the other hand, the active microcavity is fabricated by combining the silica microcavity with gain materials through several methods. One method is to fabricate the microcavity through soft glass originally doped with gain materials such as erbium (Er^{3+} ions).[27−29] For example, the Er^{3+} ion-doped tellurite glass microsphere is fabricated by the spin method, which achieves laser emission in the L-band.[27] Apart from that, the optofluidic ring resonator also acts as a microlaser platform by containing gain materials in the hollow core. The Fan group has reported a series of work on optofluidic microlasers and their biosensing applications.[30−33] Besides, gain materials such as quantum dots and rare-earth ions are directly doped into silica microcavities to achieve laser emission.[34−39] Rare-earth ions can be doped into the silica microcavity through the ion implantation method[38] and the sol−gel processing method.[34,36,37,39] An Er^{3+} ion-doped microcavity laser is experimentally demonstrated by fabricating the silica microdisk on a silicon chip, while using the ion implantation method based on a complicated CMOS process.[38] Apart from that, the sol−gel method is a low-cost and flexible way to dope rare-earth ions into the silica microcavity. The Vahala group first fabricate a silica microsphere cavity coated with the Er^{3+} ion-doped silica sol−gel film to achieve laser emission in the 1550 nm band.[34] After that, on-chip Er^{3+} ion-doped silica microtoroids are fabricated and applied in the parity-time symmetric systems.[40,41] However, the conventional sol−gel method still requires a relatively complicated process, and cracks and defects may emerge during the process, which seriously degenerates the *Q* factors of the microcavities. Therefore, so far, based on the conventional

Received: June 22, 2018
Published: July 16, 2018

DOI: 10.1021/acsphotonics.8b00838
ACS Photonics 2018, 5, 3794−3800

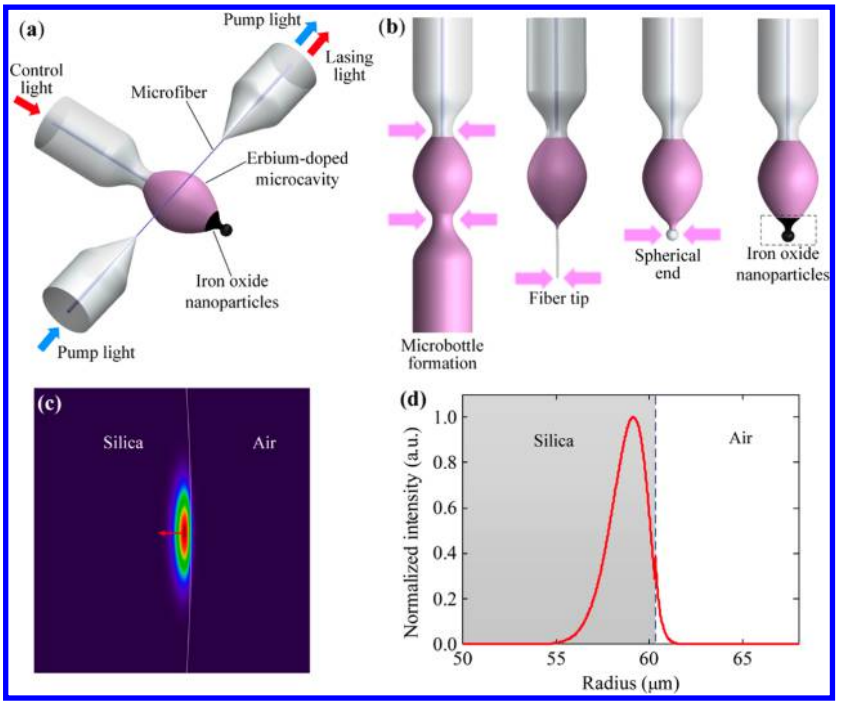

Figure 1. (a) Schematic of an all-optical tunable microlaser using the ultrahigh-Q erbium-doped hybrid microbottle cavity. Pink color represents the Er^{3+} ion doping area and black color represents the iron oxide nanoparticle coating area. (b) Fabrication process of the erbium-doped hybrid microbottle cavity coated with iron oxide nanoparticles. The pink arrow represents the CO_2 laser beam. (c) FEM simulation of the WGM field with the TM polarization in the microcavity with a radius of 60.5 μm, where the red arrow represents the electric polarization, and the white line represents the boundary between the microcavity and air. (d) WGM field profile at the cross section of the mode field center.

sol−gel method, the Q factors of the silica microcavities doped with rare-earth ions are below 10 million, which limits the microlaser performance.[19]

The wavelength tunability of the microlaser is a very important function, and the doped silica microcavity laser is tuned mainly through the aerostatic pressure method[36] and the flowing liquid induced thermal tuning method.[28] However, these methods may induce jittering of the microcavity system, and/or realize relatively limited tuning ranges. Therefore, our goal is to all-optically control the lasing wavelength in a large range, while possessing excellent microlaser performance. So far, several all-optical methods have been proposed to tune the resonance frequencies of silica WGM microcavities.[42,43] However, almost all of the reported schemes inevitably degenerate the Q factors and, accordingly, go against achieving great microlaser performance.

In this work, we propose the first all-optical tunable microlaser based on the Er^{3+} ion-doped hybrid microbottle cavity, which can avoid the above drawbacks and exhibit excellent performance. The silica microbottle cavities which are fabricated from single-mode fibers (SMFs) have been utilized in various fundamental research and practical applications.[10,26,44−46] Compared with other microcavity structures such as microspheres and microtoroids, the microbottle cavity possesses a prolate shape, which makes it support nondegenerated WGMs, whose distributions are spatially well-separated along the axial direction of the microcavity.[45,46] Therefore, it is also possible to achieve laser emission with different mode orders at different locations along the axial direction of the microcavity. As shown in Figure 1a, the pink area means that Er^{3+} ions are doped into the surface of the silica microbottle cavity. The microbottle cavity doped with Er^{3+} ions through an improved doping method possesses a Q factor of about 5.2×10^7 in the 1550 nm band. In order to excite Er^{3+} ions and achieve laser emission, the continuous-wave pump light in the 980 nm band with a line width of about 1 nm is coupled into the microcavity through the silica microfiber.[47−49] Besides, the tapered area of the microbottle is attached with a spherical end, in which iron oxide nanoparticles are coated onto its surface. Due to excellent photothermal performance of iron oxide nanoparticles, the control light fed through the axial direction of the microbottle is converted to heat and all-optical tuning of the lasing wavelength with a range of 4.4 nm is achieved.

DEVICE FABRICATION

In general, the conventional sol−gel silica film is made from a mixing solution of tetraethoxysilane (TEOS), water (H_2O), ethanol (C_2H_6O), and hydrochloric acid (HCl). During the silica film fabrication process, defects and cracks may emerge, which seriously reduce the Q factor of the microcavity. Therefore, we propose an improved and simpler method to dope Er^{3+} ions into the surface of the microcavity, while possessing the ultrahigh Q factor over 50 million. The fabrication processes are as follows: First, the Er^{3+} ion solution is made by mixing erbium nitrate hydrate ($Er(NO_3)_3{\cdot}5H_2O$), H_2O, and C_2H_6O with a weight ratio of 1.819:12.261:18.6, and the solution is shaken to be evenly distributed; Second, the polymer coating of a SMF is removed by a pincer, and then it is dipped into the Er^{3+} ion solution for several seconds; Third, the SMF attached with the Er^{3+} ion solution on its surface is fixed on the carbon dioxide laser fabrication platform; Finally, in order to further dope Er^{3+} ions into the surface of the microbottle, it is reflowed in ethanol flame. This simple method avoids the rigorous annealing process and temperature requirement. The erbium doping concentration is estimated to be around $2 \times 10^{19}/cm^3$.

DOI: 10.1021/acsphotonics.8b00838
ACS Photonics 2018, 5, 3794−3800

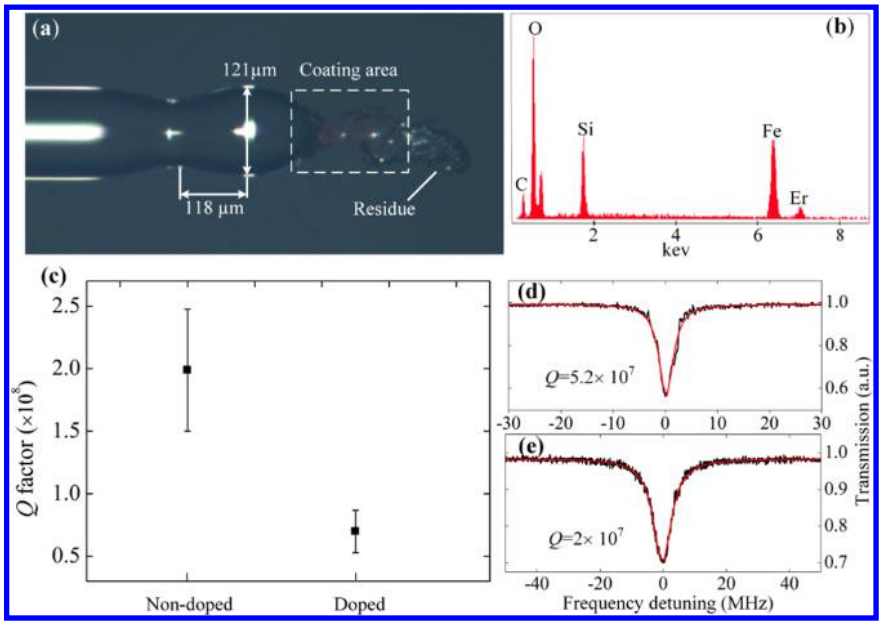

Figure 2. (a) Optical micrograph of the erbium-doped microbottle cavity coated with iron oxide nanoparticles. (b) Measured energy dispersive X-ray (EDX) spectroscopy of the coating area. (c) Measured loaded Q factors of a series of nondoped and doped microcavities. (d, e) Measured Q factors of the doped microcavities in the 1550 and 1480 nm bands, respectively, and the red lines represent Lorentz fitting.

On the basis of the above doping method, we designed a novel hybrid microbottle cavity and proposed an all-optical tuning scheme for the microcavity laser. The control light fed through the axial direction of the hybrid microbottle cavity is absorbed by iron oxide nanoparticles coated on the tapered area, which is fabricated through a dip process. Iron oxide nanoparticles can highly efficiently convert light energy into heat, which is transmitted to the WGM field locations to tune the lasing wavelength. The schematic principle and fabrication process are illustrated in Figure 1a,b. Kerosene-based iron oxide nanoparticle solution is used here. However, there may exist one problem during the dip process due to the relatively large surface tension of kerosene. When the spherical end of the microbottle is inserted into the kerosene-based iron oxide nanoparticle solution, the solution will immediately flow up along the axial direction of the microbottle and distribute at the WGM field locations. It is critical for us to control the coating area on the microcavity, especially for that with a small size. Therefore, we also propose a coating process to precisely control the coating area of iron oxide nanoparticles, which enables the hybrid microcavity to maintain the ultrahigh Q factor over 50 million. Ultraviolet (UV) curing adhesive possesses excellent viscosity, which can avoid the influence of the surface tension. The UV curing adhesive doped with iron oxide nanoparticles can be made by mixing the kerosene-based iron oxide nanoparticle solution and the optical adhesive, since these two kinds of materials are mutually soluble. The nanoparticle concentration in the UV curing adhesive is controlled by varying the mixing weight ratio between the optical adhesive and the nanoparticle solution (for details about the coating process, see part S1 in the Supporting Information). Finite element method (FEM) simulations of the WGMs are also performed to determine the mode field distributions near the surface of the microcavity.[50] The fundamental WGM with the transverse-magnetic (TM) polarization is calculated as shown in Figure 1c, and its intensity profile on the equatorial plane is also plotted in Figure 1d. The simulation result presents that about 2% of the mode field intensity is located in the evanescent field, which enables Er^{3+} ions into the surface to provide enough gain to the microlaser.

RESULTS AND DISCUSSION

Figure 2a shows the fabricated Er^{3+} ion-doped hybrid microbottle cavity with a spherical end. The area with a rough surface means that there exist mixtures of iron oxide nanoparticles and residues of the UV curing adhesive on the spherical end, that is, a tail attached on the spherical end. The microbottle cavity possesses an equatorial diameter of about 121 μm and a length of about 236 μm. The outer profile of the microbottle cavity can be fitted with a truncated harmonic oscillator profile, which can be expressed by $R(z) = R(0)[1 - (\Delta k z)^2/2]$, where $R(z)$ represents the outer radius as a function of z, Δk denotes the curvature of the microbottle geometric profile. Here, $R(0) = 60.5$ μm, $z_{max} = 118$ μm, and $\Delta k = 0.0063$ μm^{-1}. We first measure the energy dispersive X-ray spectroscopy (EDX) to demonstrate a fact that iron oxide nanoparticles are coated onto the tapered area of the microcavity, as shown in Figure 2b. There are several obvious peaks in the spectroscopy result, which represents the consistence of the atomic ratio of oxygen (O), silicon (Si), carbon (C), ferrum (Fe), and erbium (Er). Ferrum indicates that iron oxide nanoparticles are coated onto the tapered area. The existence of carbon is due to the remains of the UV curing adhesive and conductive plastic around the end, which can enhance its conductivity. The presence of erbium shows that the tapered area is also doped with Er^{3+} ions during the fabrication process. Based on the experimental test setup shown in Figure 3, we measure the Q factors of a series of doped and nondoped microbottle cavities. As shown in Figure 2c, the nondoped microbottle cavities present the ultrahigh Q factors over 10^8 in the 1550 nm band, while the doped microbottle cavities exhibit slightly lower Q factors and the highest Q factor of up to 10^8 can also be achieved. Since the improved doping method avoids the formation of cracks and defects, the degenerating Q factors are mainly due to the Er^{3+} ion absorption,[37] while without the surface defect induced

DOI: 10.1021/acsphotonics.8b00838
ACS Photonics 2018, 5, 3794−3800

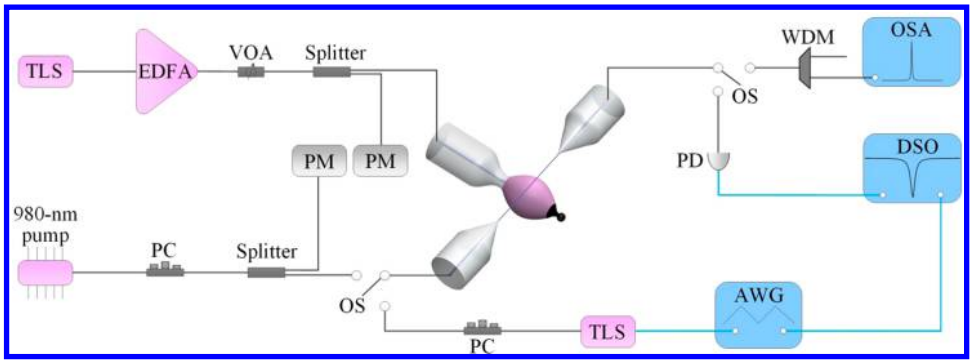

Figure 3. Experimental test setup: TLS, tunable laser source; PC, polarization controller; PD, photodetector; DSO, digital storage oscilloscope; EDFA, erbium-doped fiber amplifier; VOA, variable optical attenuator; PM, power meter; OSA, optical spectrum analyzer; WDM, wavelength division multiplexer; AWG, arbitrary waveform generator; OS, optical switch.

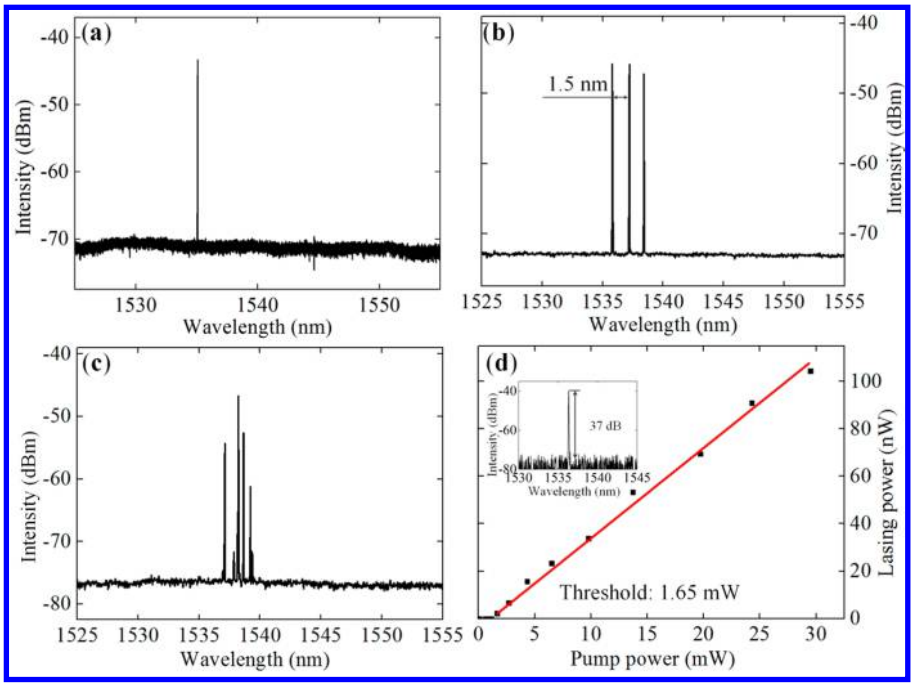

Figure 4. (a) Typical emission spectrum of the single-mode microlaser. (b) Typical emission spectrum of the multimode microlaser. The spacing between the lasing lines equals to the axial FSR. (c) Typical microlaser emission spectrum when the coupling microfiber is located away from the center area. (d) Lasing power as a function of the pump power. The inset shows a specific single-mode emission spectrum.

scattering loss. As shown in Figure 2d, based on a specifically fabricated Er^{3+} ion-doped hybrid microbottle cavity, the Q factor of about 5.2×10^7 is obtained in the 1550 nm band, which is the highest compared with those based on the conventional sol−gel method.[20,34,36,37,40,41] Furthermore, we also obtain the Q factor of about 2×10^7 in the 1480 nm band, which is a little lower than that in the 1550 nm band due to the stronger absorption of Er^{3+} ions in the 1480 nm band (for the detailed analysis of the Q factor, see part S2 in the Supporting Information).

In the case of resonant pump through a narrow-line width external-cavity laser, when the microcavity laser is tuned, the wavelength of the pump laser ought to be simultaneously tunable, which makes the experiments complicated. Therefore, a pump laser operating in the 980 nm band with a line width of about 1 nm is selected, which can cover many resonance wavelengths due to dense WGMs of the microbottle cavity.[45,46] A microfiber with a diameter of about 2 μm is fabricated from the SMF. The microfiber is first placed in the center area of the microbottle cavity. The coupling system maintains stable by enabling them to get in touch with each other. The coupling efficiency can be optimized by controlling the microfiber diameter. When the pump light is coupled into the microcavity through the evanescent field, laser emission is coupled back into the microfiber, make it can be directly measured through an optical spectrum analyzer (OSA). The lasing power is optimized by adjusting the polarization of the pump light through a polarization controller (PC). Figure 4a shows the single-mode lasing around 1535 nm, which is often observed by controlling the microfiber diameter and the coupling position. Multimode laser emission can also be observed as the location of the microfiber is slightly away from the center area, because several lasing modes with smaller axial orders are simultaneously excited,[45,46] as shown in Figure 4b. There are three periodic peaks between 1535 and 1540 nm. The measured wavelength period spacing is about 1.5 nm, which is well matched with the calculated axial free spectral range (FSR) $\Delta\lambda_q = 1.7$ nm based on $\Delta\lambda_q = \Delta k\lambda^2/2\pi n_{eff}$, where λ is the

DOI: 10.1021/acsphotonics.8b00838
ACS Photonics 2018, 5, 3794−3800

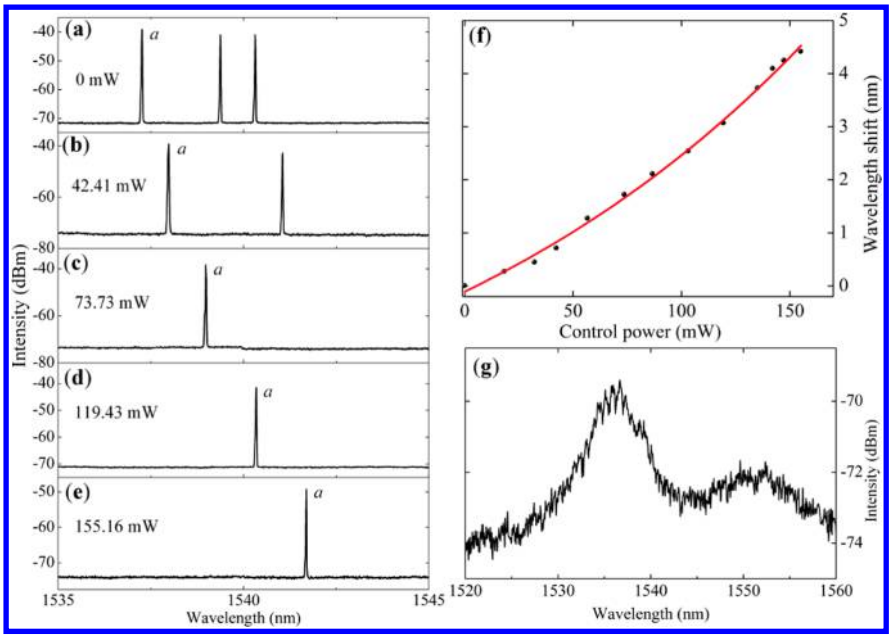

Figure 5. (a–e) Microlaser emission spectra of the erbium-doped ultrahigh-*Q* hybrid microbottle cavity at different control powers. (f) Wavelength shift of the microlaser as a function of the control power. The red line represents the fitted result. (g) Measured fluorescence spectrum of Er^{3+} ions.

wavelength in vacuum and n_{eff} is the effective refractive index. From Figure 4c, we also find that, as the microfiber location is far away from the center area, there are dense WGMs because more high-order lasing modes with large axial orders are excited and exported through the microfiber.[45,46] Therefore, based on the active microcavity, laser emission with different wavelengths can be selectively launched by placing the microfiber at different locations along the axial direction of the microbottle (for details about the selective excitation, see part S3 in the Supporting Information). Besides, it is noteworthy that the lasing power tends to decrease as the microfiber is away from the center area of the microbottle, because the mode volume is larger for the higher-order modes and the Er^{3+} ion concentration in this area is lower due to the fabrication process. The measured lasing power versus the pump power is shown in Figure 4d. We can find that as the pump power is lower than 1.65 mW, there is no laser emission. As the pump power is larger than 1.65 mW, the lasing power increases linearly with the pump power. Therefore, it is determined that the pump threshold is 1.65 mW, which is larger than those obtained through resonant pump.[20,34,37−39] However, it is the lowest among all the work through nonresonant pump,[28,36] which benefits from the ultrahigh *Q* factor of the doped microcavity. The threshold could be further decreased by optimizing the coupling efficiency between the microfiber and the microcavity.

Due to large tunability of the hybrid microbottle cavity, the lasing wavelength can be all-optical tunable. Figure 5 illustrates a fact that the lasing wavelength presents a red shift as the control power increases due to the positive thermo-optic and thermal expansion coefficients of silica.[49] By combining with Figure 5g, we find that lasing mode *a* is located near the center area of the fluorescence spectrum of Er^{3+} ions, in which the gain coefficient is the largest. With the increase of the control power, the mode number gradually decreases and the single-mode lasing is observed when the control power is 73.73 mW. It is because the gain coefficient gradually decreases in the two sides of the gain peak, and the single-mode lasing can be obtained during the tuning process. As a result, the power of lasing mode *a* also gradually decreases with the increase of the control power, because this mode always shifts to the right side of the fluorescence spectrum, which can be seen in Figure 5a–e. During the tuning process, different lasing modes may emerge and then disappear due to the mode competition.[51] However, lasing mode *a* always exists. It is noteworthy that as the control power is over 155.16 mW, lasing mode *a* disappears. Because with the shift of the lasing wavelength, the gradually decreasing gain coefficient of lasing mode *a* cannot compensate its loss. The lasing wavelength shift as a function of the control power is plotted in Figure 5f. The wavelength shift slightly nonlinearly increases with the rising control power, with an average tuning sensitivity of 30 pm/mW. When the control power increases to 155.16 mW, the maximum lasing wavelength tuning range of 4.4 nm is achieved, and it is larger than all those in the reported work on doped silica microcavity lasers.

CONCLUSION

In summary, we proposed and experimentally realized the first all-optical controllable microlaser based on the ultrahigh-*Q* Er^{3+} ion-doped hybrid microbottle cavity. By improving the Er^{3+} ion doping method, we obtained the active microbottle cavity with the *Q* factors of about 5.2×10^7 in the 1550 nm band and about 2×10^7 in the 1480 nm band, both of which are the highest compared with those obtained through the conventional sol–gel processing. Through nonresonant pump in the 980 nm band, a lasing threshold of 1.65 mW is achieved, which is lower than those in all the previous work based on the same pump method. By mixing the kerosene-based iron oxide nanoparticle solution and the UV curing adhesive, we also propose a coating process, which can enable us to precisely coat iron oxide nanoparticles onto the tapered area of the microbottle due to excellent viscosity of the optical adhesive. This enables the hybrid microcavity to maintain the ultrahigh *Q* factor, while possessing large tunability, and hence, we realize all-optical tuning of the lasing wavelength with a range of 4.4 nm. This work paves the way for future optical communications, biochemical sensing and spectroscopy.

DOI: 10.1021/acsphotonics.8b00838
ACS Photonics 2018, 5, 3794–3800

MATERIALS AND METHODS

Material Information. Kerosene-based iron oxide nanoparticle solution with the surface tension of 28×10^{-5} N/cm is purchased from Beijing Sunrise Ferro-fluid Technology Company Limited. UV curing adhesive with the viscosity of 10000 cps is purchased from Guangdong Hengda New Materials Technology Company Limited.

FEM Simulation. FEM simulations (COMSOL Multiphysics) are used to illustrate the WGM field distributions in the microbottle cavity. By building up a two-dimensional axially symmetric model, the fundamental mode distribution in the cross section of the microbottle is calculated, which is shown in Figure 1c. In order to get an acceptable accuracy, the maximum size of the mesh element is set to be about $\lambda/8$.

Experimental Test Setup. Experimental test setup is illustrated in Figure 3. Signal light derived from a narrow-line width external-cavity laser operating in the 1550 or 1480 nm band is controlled by a polarization controller (PC), and then coupled into the microcavity to excite WGMs. The transmission light exporting from the other end of the microfiber is detected by a photodetector (PD). The transmission spectrum is analyzed by a digital storage oscilloscope (DSO). Pump light coming from another laser with a line width of about 1 nm, which operates in the 980 nm band is fed into a 20/80 optical splitter, and then nonresonantly excites the Er^{3+} ion-doped microacvity and a power meter (PM) is used to detect the pump power. The lasing spectrum is measured by an optical spectrum analyzer (OSA). In order to tune the lasing wavelength, continuous-wave control light from a tunable diode laser (TLS) in the 1550 nm band is amplified by a high-power erbium-doped fiber amplifier (EDFA) and then is fed into a 10/90 optical splitter after transmitting through a variable optical attenuator (VOA). After that, the control light is fed through the axial direction of the microbottle to tune the lasing wavelength.

ASSOCIATED CONTENT

Supporting Information

The Supporting Information is available free of charge on the ACS Publications website at DOI: 10.1021/acsphotonics.8b00838.

Coating process of iron oxide nanoparticles, Q factor measurement, and selective excitation of the microbottle cavity laser (PDF).

AUTHOR INFORMATION

Corresponding Author

*E-mail: lshi@hust.edu.cn.

ORCID

Lei Shi: 0000-0002-9961-6723

Xudong Fan: 0000-0003-0149-1326

Author Contributions

S.Z. and L.S. conceived the idea. S.Z. and L.S. designed and carried out the experiments. S.Z. and B.W.X. performed the data analysis. L.S., X.D.F., and X.L.Z. discussed the results. L.S. supervised the project. All authors reviewed the manuscript.

Notes

The authors declare no competing financial interest.

ACKNOWLEDGMENTS

This work was supported by the National Natural Science Foundation of China (Grant Nos. 11774110 and 61307075), the National Key Research and Development Program of China (Grant No. 2016YFB0402503), and the State Key Laboratory of Advanced Optical Communication Systems and Networks, Shanghai Jiao Tong University, China (Grant No. 2018GZKF03002).

REFERENCES

(1) Vahala, K. J. Optical microcavities. *Nature* **2003**, *424*, 839−846.

(2) Rakovich, Y. P.; Donegan, J. F. Photonic atoms and molecules. *Laser Photonics Rev.* **2010**, *4*, 179−191.

(3) Ward, J.; Benson, O. WGM microresonators: sensing, lasing and fundamental optics with microspheres. *Laser Photonics Rev.* **2011**, *5*, 553−570.

(4) Yang, S. C.; Wang, Y.; Sun, H. D. Advances and Prospects for Whispering Gallery Mode Microcavities. *Adv. Opt. Mater.* **2015**, *3*, 1136−1162.

(5) Shen, Z.; Zhang, Y. L.; Chen, Y.; Zou, C. L.; Xiao, Y. F.; Zou, X. B.; Guo, G. C.; Dong, C. H. Experimental realization of optomechanically induced non-reciprocity. *Nat. Photonics* **2016**, *10*, 657.

(6) Chen, W. J.; Özdemir, Ş. K.; Zhao, G. M.; Wiersig, J.; Yang, L. Exceptional points enhance sensing in an optical microcavity. *Nature* **2017**, *548*, 192−196.

(7) Jiang, X. F.; Shao, L. B.; Zhang, S. X.; Yi, X.; Wiersig, J.; Wang, L.; Gong, Q. H.; Lončar, M.; Yang, L.; Xiao, Y. F. Chaos-assisted broadband momentum transformation in optical microresonators. *Science* **2017**, *358*, 344−347.

(8) Shen, X. Q.; Beltran, R. C.; Diep, V. M.; Soltani, S.; Armani, A. M. Low-threshold parametric oscillation in organically modified microcavities. *Sci. Adv.* **2018**, *4*, eaao4507.

(9) Park, Y. S.; Cook, A. K.; Wang, H. L. Cavity QED with diamond nanocrystals and silica microspheres. *Nano Lett.* **2006**, *6*, 2075−2079.

(10) Louyer, Y.; Meschede, D.; Rauschenbeutel, A. Tunable whispering-gallery-mode resonators for cavity quantum electrodynamics. *Phys. Rev. A: At., Mol., Opt. Phys.* **2005**, *72*, 031801.

(11) Zhi, Y. Y.; Yu, X. C.; Gong, Q. H.; Yang, L.; Xiao, Y. F. Single nanoparticle detection using optical microcavities. *Adv. Mater.* **2017**, *29*, 1604920.

(12) Heylman, K. D.; Knapper, K. A.; Horak, E. H.; Rea, M. T.; Vanga, S. K.; Goldsmith, R. H. Optical microresonators for sensing and transduction: a materials perspective. *Adv. Mater.* **2017**, *29*, 1700037.

(13) Toren, P.; Ozgur, E.; Bayindir, M. Real-time and selective detection of single nucleotide DNA mutations using surface engineered microtoroids. *Anal. Chem.* **2015**, *87*, 10920−10926.

(14) Lu, T.; Lee, H.; Chen, T.; Herchak, S.; Kim, J. H.; Fraser, S. E.; Flagan, R. C.; Vahala, K. J. High sensitivity nanoparticle detection using optical microcavities. *Proc. Natl. Acad. Sci. U. S. A.* **2011**, *108*, 5976−5979.

(15) Forstner, S.; Sheridan, E.; Knittel, J.; Humphreys, C. L.; Brawley, G. A.; Dunlop, H. R.; Bowen, W. P. Ultrasensitive optomechanical magnetometry. *Adv. Mater.* **2014**, *26*, 6355−6355.

(16) Salehzadeh, O.; Djavid, M.; Tran, N. H.; Shih, I.; Mi, Z. Optically pumped two-dimensional MoS_2 lasers operating at room-temperature. *Nano Lett.* **2015**, *15*, 5302−5306.

(17) Reed, J. C.; Zhu, A. Y.; Zhu, H.; Yi, F.; Cubukcu, E. Wavelength tunable microdisk cavity light source with a chemically enhanced MoS_2 emitter. *Nano Lett.* **2015**, *15*, 1967−1971.

(18) Reynolds, T.; Riesen, N.; Meldrum, A.; Fan, X. D.; Hall, J. M. M.; Monro, T. M.; Francois, A. Fluorescent and lasing whispering gallery mode microresonators for sensing applications. *Laser Photonics Rev.* **2017**, *11*, 1600265.

(19) He, L. N.; Özdemir, Ş. K.; Yang, L. Whispering gallery microcavity lasers. *Laser Photonics Rev.* **2013**, *7*, 60−82.

(20) Yang, L.; Armani, D. K.; Vahala, K. J. Fiber-coupled erbium microlasers on a chip. *Appl. Phys. Lett.* **2003**, *83*, 825−826.

DOI: 10.1021/acsphotonics.8b00838
ACS Photonics 2018, 5, 3794−3800

(21) Li, B. B.; Clements, W. R.; Yu, X. C.; Shi, K.; Gong, Q. H.; Xiao, Y. F. Single nanoparticle detection using split-mode microcavity Raman lasers. *Proc. Natl. Acad. Sci. U. S. A.* **2014**, *111*, 14657−14662.
(22) Spillane, S. M.; Kippenberg, T. J.; Vahala, K. J. Ultralow-threshold Raman laser using a spherical dielectric microcavity. *Nature* **2002**, *415*, 621−623.
(23) Chembo, Y. K.; Grudinin, I. S.; Yu, N. Spatiotemporal dynamics of Kerr-Raman optical frequency combs. *Phys. Rev. A: At., Mol., Opt. Phys.* **2015**, *92*, 043818.
(24) Kippenberg, T. J.; Spillane, S. M.; Min, B.; Vahala, K. J. Theoretical and experimental study of stimulated and cascaded Raman scattering in ultrahigh-Q optical microcavities. *IEEE J. Sel. Top. Quantum Electron.* **2004**, *10*, 1219−1228.
(25) Dong, C. H.; Shen, Z.; Zou, C. L.; Zhang, Y. L.; Fu, W.; Guo, G. C. Brillouin-scattering-induced transparency and non-reciprocal light storage. *Nat. Commun.* **2015**, *6*, 6193.
(26) Asano, M.; Takeuchi, Y.; Ozdemir, S. K.; Ikuta, R.; Yang, L.; Imoto, N.; Yamamoto, T. Stimulated Brillouin scattering and Brillouin-coupled four-wave-mixing in a silica microbottle resonator. *Opt. Express* **2016**, *24*, 12082−12092.
(27) Peng, X.; Song, F.; Jiang, S.; Peyghambarian, N.; Kuwata-Gonokami, M.; Xu, L. Fiber-taper-coupled L-band Er^{3+}-doped tellurite glass microsphere laser. *Appl. Phys. Lett.* **2003**, *82*, 1497.
(28) Ward, J. M.; Yang, Y.; Chormaic, S. N. Glass-on-glass fabrication of bottle-shaped tunable microlasers and their applications. *Sci. Rep.* **2016**, *6*, 25152.
(29) Fang, Z. J.; Chormaic, S. N.; Wang, S. Y.; Wang, X.; Yu, J. B.; Jiang, Y. X.; Qiu, J. R.; Wang, P. F. Bismuth-doped glass microsphere lasers. *Photonics Res.* **2017**, *5*, 740−744.
(30) Fan, X. D.; Yun, S. H. The potential of optofluidic biolasers. *Nat. Methods* **2014**, *11*, 141−147.
(31) Chen, Y. C.; Chen, Q. S.; Fan, X. D. Lasing in blood. *Optica* **2016**, *3*, 809−815.
(32) Kiraz, A.; Chen, Q. S.; Fan, X. D. Optofluidic lasers with aqueous quantum dots. *ACS Photonics* **2015**, *2*, 707−713.
(33) Sun, Y. Z.; Shopova, S. I.; Wu, C. S.; Arnold, S.; Fan, X. D. Bioinspired optofluidic FRET lasers via DNA scaffolds. *Proc. Natl. Acad. Sci. U. S. A.* **2010**, *107*, 16039−16042.
(34) Yang, L.; Vahala, K. J. Gain functionalization of silica microresonators. *Opt. Lett.* **2003**, *28*, 592−594.
(35) Grivas, C.; Li, C. Y.; Andreakou, P.; Wang, P. F.; Ding, M.; Brambilla, G.; Manna, L.; Lagoudakis, P. Single-mode tunable laser emission in the single-exciton regime from colloidal nanocrystals. *Nat. Commun.* **2013**, *4*, 2376.
(36) Yang, Y.; Lei, F. C.; Kasumie, S.; Xu, L. H.; Ward, J. M.; Yang, L.; Chormaic, S. N. Tunable erbium-doped microbubble laser fabricated by sol-gel coating. *Opt. Express* **2017**, *25*, 1308−1313.
(37) Jiang, X. F.; Xiao, Y. F.; Zou, C. L.; He, L. N.; Dong, C. H.; Li, B. B.; Li, Y.; Sun, F. W.; Yang, L.; Gong, Q. H. Highly Unidirectional Emission and Ultralow-Threshold Lasing from On-Chip Ultrahigh-Q Microcavities. *Adv. Mater.* **2012**, *24*, OP260−OP264.
(38) Kippenberg, T. J.; Kalkman, J.; Polman, A.; Vahala, K. J. Demonstration of an erbium-doped microdisk laser on a silicon chip. *Phys. Rev. A: At., Mol., Opt. Phys.* **2006**, *74*, 051802.
(39) Ding, Y.; Fan, H. B.; Zhang, X.; Jiang, X. S.; Xiao, M. Ultralow-threshold neodymium-doped microsphere lasers on a silicon chip. *Opt. Commun.* **2017**, *395*, 51−54.
(40) Peng, B.; Özdemir, Ş. K.; Lei, F. C.; Monifi, F.; Gianfreda, M.; Long, G. L.; Fan, S. H.; Nori, F.; Bender, C. M.; Yang, L. Parity-time-symmetric whispering-gallery microcavities. *Nat. Phys.* **2014**, *10*, 394−398.
(41) Chang, L.; Jiang, X. S.; Hua, S. Y.; Yang, C.; Wen, J. M.; Jiang, L.; Li, G. Y.; Wang, G.; Xiao, M. Parity-time symmetry and variable optical isolation in active-passive-coupled microresonators. *Nat. Photonics* **2014**, *8*, 524−529.
(42) Liu, Y.; Shi, L.; Xu, X. B.; Zhao, P.; Wang, Z. Q.; Pu, S. L.; Zhang, X. L. All-optical tuning of a magnetic-fluid-filled optofluidic ring resonator. *Lab Chip* **2014**, *14*, 3004−3010.
(43) Bo, F.; Wang, J.; Cui, J.; Ozdemir, S. K.; Kong, Y.; Zhang, G.; Xu, J.; Yang, L. Lithium-Niobate-Silica Hybrid Whispering-Gallery-Mode Resonators. *Adv. Mater.* **2015**, *27*, 8075−8081.
(44) Asano, M.; Takeuchi, Y.; Chen, W. J.; Özdemir, Ş. K.; Ikuta, R.; Imoto, N.; Yang, L.; Yamamoto, T. Observation of optomechanical coupling in a microbottle resonator. *Laser Photonics Rev.* **2016**, *10*, 603−611.
(45) Pöllinger, M.; O'Shea, D.; Warken, F.; Rauschenbeutel, A. Ultrahigh-Q tunable whispering-gallery-mode microresonator. *Phys. Rev. Lett.* **2009**, *103*, 053901.
(46) Murugan, G. S.; Wilkinson, J. S.; Zervas, M. N. Selective excitation of whispering gallery modes in a novel bottle microresonator. *Opt. Express* **2009**, *17*, 11916−11925.
(47) Zhao, P.; Shi, L.; Liu, Y.; Wang, Z. Q.; Zhang, X. L. Compact in-line optical notch filter based on an asymmetric microfiber coupler. *Appl. Opt.* **2013**, *52*, 8834−8839.
(48) Wang, K. Y.; Gu, Z. Y.; Sun, W. Z.; Li, J. K.; Xiao, S. M.; Song, Q. H. Quasi-guiding Modes in Microfibers on a High Refractive Index Substrate. *ACS Photonics* **2015**, *2*, 1278−1283.
(49) Zhao, P.; Shi, L.; Liu, Y.; Wang, Z. Q.; Pu, S. L.; Zhang, X. L. Iron-oxide nanoparticles embedded silica microsphere resonator exhibiting broadband all-optical wavelength tunability. *Opt. Lett.* **2014**, *39*, 3845−3848.
(50) Zhang, C.; Zou, C. L.; Yan, Y. L.; Wei, C.; Cui, J. M.; Sun, F. W.; Yao, J. N.; Zhao, Y. S. Self-Assembled Organic Crystalline Microrings as Active Whispering-Gallery-Mode Optical Resonators. *Adv. Opt. Mater.* **2013**, *1*, 357−361.
(51) Feng, L.; Wong, Z. J.; Ma, R. M.; Wang, Y.; Zhang, X. Single-mode laser by parity-time symmetry breaking. *Science* **2014**, *346*, 972−975.

DOI: 10.1021/acsphotonics.8b00838
ACS Photonics 2018, 5, 3794−3800